

科学研究費助成事業 研究成果報告書

平成 30 年 6 月 22 日現在

機関番号：13801

研究種目：基盤研究(C) (一般)

研究期間：2015～2017

課題番号：15K04637

研究課題名(和文) Infrared micro-sensor based on 3D photonic crystal

研究課題名(英文) Infrared micro-sensor based on 3D photonic crystal

研究代表者

MIZEIKIS Vyganta (Mizeikis, Vygantas)

静岡大学・電子工学研究所・教授

研究者番号：50374666

交付決定額(研究期間全体)：(直接経費) 3,900,000円

研究成果の概要(和文)：本研究では、3次元フォトニック結晶による新規赤外センサの開発を目的としている。一般的には、半導体ベースの赤外領域に感度を有するフォトダイオードなどの光検出器が用いられる。しかしこの一般的な方法では高純度な半導体を用いて、クリーンルームや真空環境下にてプロセスをする必要がある。本研究において、赤外感度を示す微小フォトニック結晶構造を普通の研究室環境で迅速に作製することができた。フォトニック結晶をベースとしたセンサは光学読み出し可能なため、従来センサの電気ノイズ特性フリーである。本手法は、今後生体や医療、セキュリティ応用に向けた赤外センシングやイメージングに貢献するものと期待される。

研究成果の概要(英文)：This study focused on realization of new kind of infrared sensor based on 3D photonic crystal. Ordinary infrared sensors based on semiconductors can produce infrared-sensitive photodetectors, such as photodiodes. However, this approach requires high purity semiconductors and their processing using advanced equipment in cleanroom and vacuum conditions. In this study, small infrared-sensitive photonic crystal structures were realized quickly in an ordinary laboratory environment. The sensors are optically readable, and therefore are free of electrical noise characteristic to traditional sensors. Their application may contribute to infrared sensing and imaging used in biological, medical, and security applications.

研究分野：応用光学

キーワード：optical sensors photonic crystals infrared sensors structural color direct laser writing
laser fabrication

1. 研究開始当初の背景

赤外光領域の応用研究において、赤外光検出器の低感度、高熱容量、応答速度制限、赤外ポロメータ検出器の作製時間など様々な制約が課題であった。

Conventional infrared (IR) sensors exploit electronic response of narrow-gap semiconductors, or bolometric response of materials. However, fabrication of semiconductor-based IR detectors often requires advanced semiconductor growth and micro/nano-fabrication techniques, while their high sensitivity operation requires external cooling. Traditional bolometric sensors have large size and considerable thermal mass, which limits their response speed.

2. 研究の目的

本研究目的は、構造色を示す人工フォトニック結晶構造によるポロメータ検出感度の改善である。

It was suggested recently that optical response of 3D nanostructured dielectrics can be exploited for IR detection[1]. Such detectors would be more compact, have faster response time, and higher sensitivity than traditional bolometric detectors. The optical response concerned here is related to the structural color phenomenon found in naturally existing dielectric systems having nanoscale periodicity, such as gemstone opals, wings of some bugs and butterflies, fish scales, etc. [2] that are similar to the naturally existing photonic crystals (PhC). Structural color originates from photonic band gap (PBG) or photonic stop-gap (PSG) reflectivity band of the PhC. It was demonstrated some time ago that color of blue scales covering wings of Morpho butterflies (reflectance band centered on the visible wavelengths around 450nm

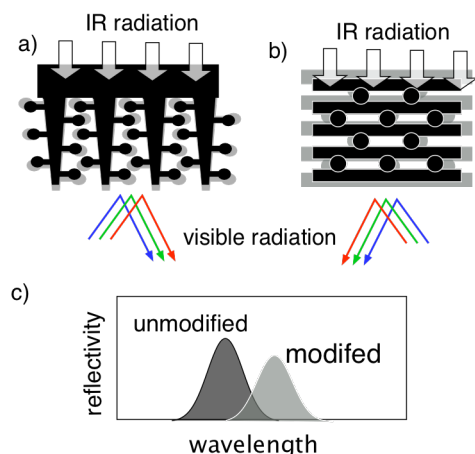


Figure 1. Schematic mechanism of IR sensitivity in Morpho butterfly wing (a), artificial PhC (b), modification of optical reflectivity due to IR absorption (c).

can be modified by IR radiation absorbed in the chitine, a protein composing the scales. IR absorption leads to heating and thermal expansion of the PhC lattice, and a change in the PSG optical reflectivity as is explained in Fig. 1(a-c).

3. 研究の方法

レーザー直接描画方により 3次元フォトニック結晶を作製し、作製構造の光学特性等を評価する。

Practical replication of structural color materials is of considerable practical interest for various applications[3], including IR sensing. However, it requires

fabrication of 3D PhC structures with PBG/PSG spectral regions at visible wavelengths, which is very challenging using natively 2D planar lithography and semiconductor nano-processing techniques.

In this study we have used using femtosecond Direct Laser Write (DLW) technique[4] for realization of 3D PhC structures exhibiting structural color, which is controllable in a wide range of wavelengths corresponding to the color range from red to blue, depending on the PhC lattice period and dielectric filling ratio. This approach provides a useful route to obtain porous dielectrics exhibiting structural color, for applications in PhC-based IR optical sensors.

Optical setup used for the DLW experiments is schematically shown in Fig.2(a). The laser source for DLW was a femtosecond oscillator with a temporal pulse length of 100fs, a central wavelength of 800nm, and a repetition rate of 80MHz. The laser beam was attenuated/switched by an acousto-optical modulator (AOM) and focused into the bulk of photoresist film by an oil-immersion microscope objective lens with a numerical aperture NA=1.35. Laser writing was facilitated by translating the sample, which was mounted on a computer-controlled three-dimensional translation stage along a preset trajectory. To ensure a proper non-linear exposure of photoresist at the focus, and a sufficient resolution of the DLW, stage translation speed was typically set in the range of 50-100 μ m/s, while average laser power at the focus was around 2mW. *In situ* observation of the fabrication process employed a light-emitting diode illuminator, and a video camera.

4. 研究成果

3D woodpile photonic crystal architecture[5] is explained schematically in Fig. 2(b). The structure is built from dielectric rods, arranged into layers and stacked vertically. In all fabricated samples fixed ratio between the in-plane and vertical lattice periods, denoted as a_{xy} and a_z respectively, was

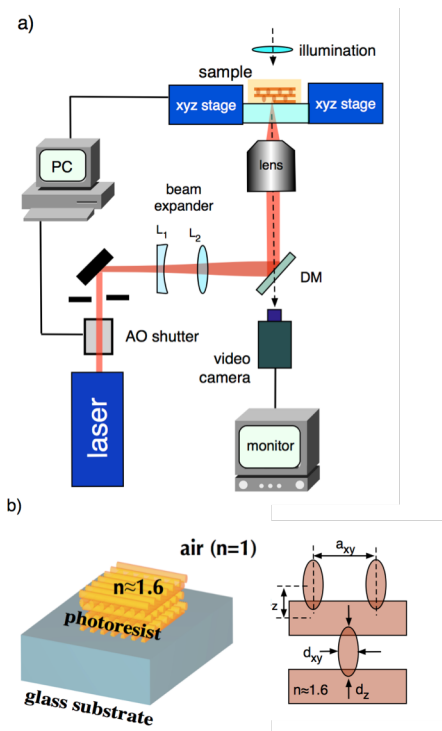


Figure 2. Experimental DLW setup (a), schematic explanation of 3D woodpile structure on a glass substrate and its geometrical parameters (b).

maintained such that $a_z \approx 0.35a_{xy}$, and symmetry of the PhC unit cell was close to face-centered cubic (fcc). Cross sectional shape of the woodpile rods is elliptical due to inherent elongation of two-photon point-spread function at the focus of the writing laser beam. For the focusing direction along the vertical axis (i.e., normal to the woodpile planes) and NA of the lens used, ratio between the minor (in-plane) and major (vertical) diameters of the ellipse, denoted as d_{xy} and d_z respectively, was $d_z/d_{xy} \approx 2.7$.

Structural characterization of the fabricated samples was performed using Scanning Electron Microscopy (SEM). Optical reflectivity spectra of the samples were measured using a home-made micro-reflectivity setup at visible wavelengths, and a Fourier-Transform Infra-Red (FTIR) micro-spectrometer.

The initial samples for DLW used negative-tone Zr-containing hybrid organic-inorganic photoresist SZ2080 intended for 3D laser lithography applications [6]. Prior to DLW, the resist was drop-cast and dried on a microscope cover glass substrates (thickness of about 180 μm). During the DLW, the laser beam was focused into photoresist through the glass substrate as shown in Fig. 2. The exposed samples were developed and dried.

According to the Maxwell's scaling behavior[7] frequency of photonic bands, PSGs, and other characteristic features in a PhC band diagram is proportional to the PhC lattice period and inversely

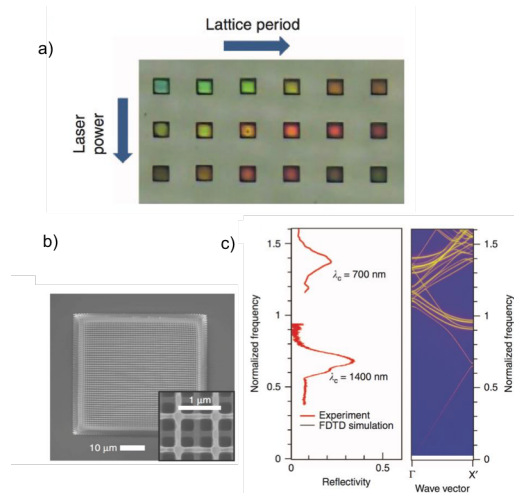


Figure 3. Structural color and its origin, (a) optical microscopy images of several samples with different lattice parameters, (b) SEM image of a selected PhC structure, (c) comparison between the measured sample reflectivity and the simulated photonic band diagram.

proportional to the average refractive index. Design value of the PhC lattice period is set directly during DLW, while average refractive index depends on the dielectric filling ratio in the structure, which is controlled indirectly by adjusting the average laser power and the size the optically exposed region at the focus of the writing beam.

Figure 3 summarizes structural and optical properties of the fabricated woodpile PhC samples exhibiting structural color. The samples in the array in Fig. 3(a) have the same footprint area of $(25 \times 25) \mu\text{m}^2$, and the same number of layers $N = 20$, but their in-plane lattice period a_{xy} and the fabricating laser power P_{las} increase from $a_{xy} = 700$ nm and $P_{\text{las}} = 1.9$ mW, with increments of 50 nm and 0.1 mW, respectively, starting from the origin point of the array (bottom-left corner). Bright color dependent on the lattice period and average laser power can be seen, and exhibits a red shift with increasing lattice period and writing laser power (that is, dielectric filling ratio) in qualitative agreement with Maxwell's scaling behavior, thus indicating that its origin is linked to the periodicity of the PhC. Scanning electron microscopy (SEM) images shown in Fig. 3(b) for one sample demonstrate high quality and high spatial resolution of DLW fabrication. Woodpile rods have lateral thickness $a_{xy} = 135$ nm, while its in-plane lattice period (distance between two neighboring woodpile rods), designed to be 1000 nm, is reduced to 940 nm due to shrinkage of the PhC lattice by a relative amount of 5%. Fig. 3(c) summarizes interpretation of the physical

mechanism of structural color by comparing the experimental reflectivity spectrum of the PhC structure shown in Fig. 3(b) with photonic band diagram simulated using finite-difference time-domain (FDTD) technique. As can be seen from the band diagram, a fundamental PSG opens along the observation (woodpile layer stacking) direction at the wavelength of 1400 nm wavelength. Thus, fundamental PSG as a source of structural color can be ruled out. However, the visible reflectivity band occurring near the 700 nm spectrally overlaps with regions in the band diagram containing high density of nearly horizontal high-order photonic bands, known to have a low group velocity, and to exhibit a strong back-scattering. It can be concluded, that resonant backscattering should be associated with coupling losses between incident plane waves and slow-light modes inside the PhC[8]. Hence, this study has demonstrated that exploitation of high-order photonic band dispersion allows realization of PhC-based structural color materials without the need to downscale their lattice period.

SEM data in Fig. 3(b) shows that PhC structures are non-uniform due to the photoresist shrinkage. This is evident from the bottom plane (attached to the glass substrate) being visibly wider than the top plane of woodpile PhC. Non-uniform deformation distorts clarity and intensity of the structural color, but during the experiments it was difficult to avoid photoresist shrinkage, especially when woodpile rods become thin approaching the diameter of 100 nm. To avoid this problem, PhC samples were fabricated not attached to the substrate using cages consisting of four massive photoresist rods attached to the substrate, and connected by a ring at the top, as shown schematically in Fig. 4(a). This geometry allows uniform shrinkage/swelling and ensures thermal and mechanical isolation of the PhCs from the substrate. As a result, more intense, and environmentally sensitive structural color can be expected, as is evidenced by the optical microscopy images shown in Fig. 4(b). As can be seen, the structures exhibit more intense colors in a wider spectral range range. Fig. 4(c) shows reflectivity spectra of several selected PhCs from the previous panel. Spectral position of the reflectance peak wavelength is correlated with the visible color of these samples.

In summary, porous dielectric structures with woodpile photonic crystal architecture were fabricated by femtosecond direct laser write lithography in photoresist and characterized, structurally and optically. The fabricated samples were found to exhibit resonant high-reflectance bands at visible wavelengths depending on the lattice parameters. Experimental and theoretical characterisation of the samples have indicated that the structural colour occurs due to strong optical reflectivity associated with slow light in the PhC.

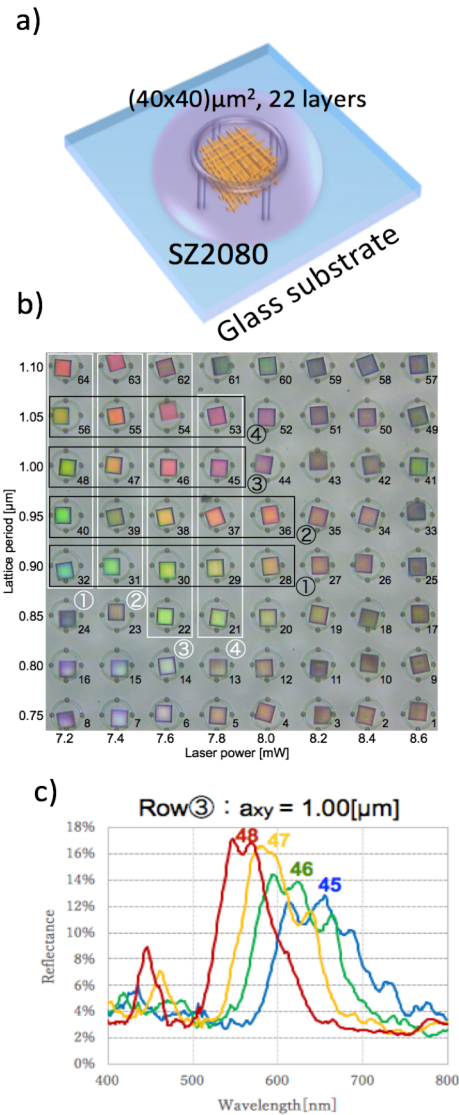


Figure 4. Coloration in uniform PhCs. (a) schematic explanation of encaged woodpile geometry, the woodpile and cage are shown inside the droplet of photoresist, i.e., prior to development, (b) optical microscopy images of PhCs with different lattice periods fabricated using different laser powers indicated in the Figure, (c) optical reflectivity spectra of several PhCs from the previous panel.

This finding has one attractive feature for future applications. Since high-frequency photonic bands are responsible for the slow light effect, central frequency of the high reflectivity region is relatively high. As a consequence, it is possible to obtain strong reflectivity bands at visible wavelengths without the need to severely downscale the lattice period. The floating PhC structures realized in this study can be used for IR sensing applications in a similar manner as the natural scales of Morpho butterfly, and become

building blocks of novel IR sensing and imaging devices.

- [1]. D. Pris *et al.* Nature Photonics 6, 195–200 (2012).
- [2]. S. Kinoshita *et al.*, Rep. Prog. Phys. 71, 076401 (2008).
- [3]. A.Saito *et al.* J. Nanosci Nanotechnol. 11, 2785–2792 (2011).
- [4]. S. Juodkasis, V. Mizeikis, H. Misawa, J. Appl. Phys. 106, 051101 (2009).
- [5]. K. M. Ho *et al.*, Solid State Commun. 89, 413–416 (1994).
- [6]. A. Ovsiannikov *et al.* Laser Chem.2008, ID 493059, (2008).
- [7]. J. D. Joannopoulos *et al.* Photonic Crystals: Molding the Flow of Light, Princeton University Press, Princeton, (2008).
- [8]. M. Malinauskas *et al.* Light:Sci.&Appl. 5, p. e16133 (2016).

5. 主な発表論文等

(研究代表者、研究分担者及び連携研究者には下線)

〔雑誌論文〕(計 6 件)

- (1) Ryu M, Hobayashi H, Balcytis A, Wang X, Vongsvivut J, Li J, Urayama N, Mizeikis V, Tobin M, Juodkasis S, Nanoscale chemical mapping of laser-solubilized silk、Mater. Res. Express、査読有、 Vol. 4 No. 11、2017、p. 115028、DOI: 10.1088/2053-1591/aa98a9
- (2) Faniayeu I, Khakhomov S, Semchenko I, Mizeikis V、Highly transparent twist polarizer metasurface、Appl. Phys. Lett.、査読有、 Vol. 111 No. 11、2017、p. 111108、DOI: 10.1063/1.4994777
- (3) Faniayeu I, Mizeikis V、Realization of a helix-based perfect absorber for IR spectral range using the direct laser write technique、Opt Mater. Express、査読有、 Vol. 7 No. 5、2017、pp. 1453-1462、DOI:10.1364/OME.7.001453
- (4) Faniayeu I, Mizeikis V、Vertical split-ring resonator perfect absorber metamaterial for IR frequencies realized via femtosecond direct laser writing、Appl. Phys. Express、査読有、 Vol. 10、2017、p. 062001、DOI: 10.7567/APEX.10.062001
- (5) Rekstyte S, Jonavičius T, Gailevicius D, Malinauskas M, Mizeikis V, Gamaly E G, Juodkasis S、Nanoscale Precision of 3D Polymerization via Polarization Control、Adv. Opt. Mater.、査読有、 Vol. 4、2016、pp. 1209-1214、DOI: 10.1002/adom.201600155
- (6) Paipulas D, Buividas R, Juodkasis S, Mizeikis V、Local Photorefractive Modification in Lithium Niobate Using

Ultrafast Direct Laser Write Technique、J. Laser Micro-Nano Eng.、査読有、 Vol. 11、2016、pp. 246-252、DOI: 10.2961/jlmm.2016.02.0016

〔学会発表〕(計 7 件)

- (1) Faniayeu I, Mizeikis V、Realization of 3D Metamaterial Perfect Absorber Structures by Direct Laser Writing、SPIE Photonics West 2017 (2017).
- (2) Mizeikis V, Faniayeu I, Rekstyte S, Staliunas K, Juodkasis S、Tailoring of Micro-/Nano-Photonic Structures by 3D Laser Lithography、ICMAT 2017 (2017)
- (3) Gailevicius D, Jonusauskas L, Sakalauskas D, Sakirzanovas S, Gadonas R, Juodkasis S, Mizeikis V, Staliunas K, Malinauskas M, Down-scaling of organic-inorganic 3D polymer lattices through pyrolysis、LPM 2017 (2017)
- (4) Faniayeu I, Mizeikis V、Tailoring of 3D optical perfect absorber metamaterials using direct laser write technique、LPM 2017 (2017)
- (5) Rekstyte S, Paipulas D, Malinauskas M, Mizeikis V、Reversible deformations of laser-written 3D photoresist structures、LPM 2017 (2017)
- (6) Mizeikis V, Hayran Z, Kurt H, Gailevicius D, Malinauskas M, Juodkasis S, Staliunas K、Fabrication of optical field concentrators based on 3D chirped photonic crystals by direct laser writing technique、META 2017 (2017)
- (7) Mizeikis V, Faniayeu I、Laser fabrication of perfect absorbers、SPIE NanoPhotonics Australasia 2017 (2017)

〔図書〕(計 0 件)

〔産業財産権〕

○出願状況 (計 0 件)

名称：
発明者：
権利者：
種類：
番号：
出願年月日：
国内外の別：

○取得状況 (計 0 件)

名称：
発明者：
権利者：
種類：
番号：

取得年月日：

国内外の別：

〔その他〕

ホームページ等

無し

6. 研究組織

(1)研究代表者

MIZEIKIS Vygantas (MIZEIKIS, Vygantas)

静岡大学電子工学研究所・教授

研究者番号：50374666

(2)研究分担者

無し

(3)連携研究者

無し

(4)研究協力者

無し